

**Degradation rates of benzotriazoles and benzothiazoles under UV-C
irradiation and the advanced oxidation process UV/H₂O₂**

Sabrina Bahn Müller^{†,‡}, Urs von Gunten^{†,‡,§}, Clara H. Loi[&], Kathryn L. Linge[&], and Silvio
Canonica^{*†}

[†]Eawag, Swiss Federal Institute of Aquatic Science and Technology
CH-8600, Dübendorf, Switzerland

[‡]Institute of Biogeochemistry and Pollutant Dynamics, ETH Zürich,
CH-8092, Zürich, Switzerland

[§]School of Architecture, Civil and Environmental Engineering (ENAC),
Ecole Polytechnique Fédérale de Lausanne (EPFL),
CH-1015 Lausanne, Switzerland

[&]Curtin Water Quality Research Centre, Department of Chemistry, Curtin University
GPO Box U1987, Perth, Western Australia 6845, Australia

*To whom correspondence should be addressed.

E-mail: silvio.canonica@eawag.ch

Phone: +41-58-765-5453

This document is the accepted manuscript version of the following article:
Bahn Müller, S., Loi, C. H., Linge, K. L., von Gunten, U., & Canonica, S. (2015). Degradation rates
of benzotriazoles and benzothiazoles under UV-C irradiation and the advanced oxidation process UV/
H₂O₂. *Water Research*, 74, 143-154. <https://doi.org/10.1016/j.watres.2014.12.039>

This manuscript version is made available under the CC-BY-NC-ND 4.0
license <http://creativecommons.org/licenses/by-nc-nd/4.0/>

Abstract

Benzotriazoles (BTs) and benzothiazoles (BTHs) are extensively used chemicals found in a wide range of household and industrial products. They are chemically stable and are therefore ubiquitous in the aquatic environment. The present study focuses on the potential of ultraviolet (UV) irradiation, alone or in combination with hydrogen peroxide (H_2O_2), to remove BTs and BTHs from contaminated waters. Six compounds, three out of each chemical class, were investigated using a low-pressure mercury lamp (main emission at 254 nm) as the radiation source. Initially, the direct phototransformation kinetics and quantum yield in dilute aqueous solution was studied over the pH range of 4–12. All BTs and BTHs, except for benzothiazole, exhibited pH-dependent direct phototransformation rate constants and quantum yields in accordance to their acid–base speciation ($7.1 < \text{p}K_{\text{a}} < 8.9$). The direct phototransformation quantum yields (9.0×10^{-4} – 3.0×10^{-2} mol einstein⁻¹), as well as the photon fluence-based rate constants (1.2 – 48 m² einstein⁻¹) were quite low. This suggests that UV irradiation alone is not an efficient method to remove BTs and BTHs from impacted waters. The second-order rate constants for the reaction of selected BTs and BTHs with the hydroxyl radical were also determined, and found to fall in the range of 5.1 – 10.8×10^9 M⁻¹s⁻¹, which is typical for aromatic contaminants. Finally, the removal of BTs and BTHs was measured in wastewater and river water during application of UV irradiation or the advanced oxidation process UV/ H_2O_2 . The latter process provided an efficient removal, mostly due to the effect of the hydroxyl radical, that was comparable to other aromatic aquatic contaminants, in terms of energy requirement or treatment costs.

Keywords: Photolysis; Quantum yield; Hydroxyl radical; AOP; UV fluence.

1. Introduction

Benzotriazoles (BTs) and benzothiazoles (BTHs) are high production chemicals used in industrial and household products. Benzotriazoles are used as corrosion inhibitors in aircraft de-icing/anti-icing fluids (Cancilla et al., 1998, Cancilla et al., 2003a, Cancilla et al., 2003b), as dishwasher agents for silver protection (Janna et al., 2011), in cooling and hydraulic fluids and as ultraviolet (UV) stabilizers (De Orsi et al., 2006). The basic chemical structure of BTs (Table 1) consists of a five-membered ring with three nitrogen atoms sharing a C–C bond with a benzene ring. Benzotriazoles are characterized by a high water solubility, high polarity and low sorption tendency, due to their low octanol-water partition coefficients ($\log K_{OW} = 1.23\text{--}2.17$) (Hart et al., 2004). Therefore they are expected to be very mobile in the aquatic environment. Furthermore, BTs are weak acids ($pK_a = 7.5\text{--}8.8$), which should be considered to assess their chemical reactivity. In addition to their known chemical stability, BTs were considered to be resistant towards microbial transformation (Hem et al., 2003), but recent studies have proposed that BTs are slowly degraded by microorganisms under aerobic conditions in activated sludge (Huntscha et al., 2012, Liu et al., 2011).

Benzothiazoles are used as vulcanization accelerators in the manufacture of rubber products and tires (Engels H.-W., 1993), as herbicides in agriculture (Hartley and Kidd, 1987), as fungicides in the leather and lumber production (Bugby et al., 1990, Kennedy, 1986) and as stabilizers in the photo industry (Wik and Dave, 2009). The chemical structure of BTHs (Table 1) consists of a 5-membered 1,3-thiazole ring attached to a benzene ring by a common C–C bond. Benzothiazoles are less water soluble than BTs, though they also exhibit low octanol-water partition coefficients ($\log K_{OW} = 1.99\text{--}2.41$) (Brownlee et al., 1992), suggesting that BTHs are not prone to bioaccumulate or sorb to particles (Reddy and Quinn, 1997). Consequently, once they have

entered the aquatic environment, they will tend to stay in the aqueous phase. It has been reported that BTHs are to some degree microbially degradable, but their transformation rate is low (Reddy and Quinn, 1997, Reemtsma et al., 1995).

(Table 1)

Benzotriazoles and BTHs are reported to be poorly eliminated by conventional wastewater treatment processes (Kloepfer et al., 2005, Reemtsma et al., 2010, Weiss et al., 2006). Hence, wastewater effluent discharge is one of their main pathways into the aquatic environment. Additional sources of BTs include runoff due to the application of aircraft de-icing/anti-icing fluids (Cancilla et al., 2003b) and, for BTHs, street runoff containing abrasion residues of tires (Fries et al., 2011). As a result of their widespread application and their resistance towards abiotic and partly biotic transformation, BTs and BTHs have been detected regularly in wastewaters (Fries et al., 2011, Voutsas et al., 2006), surface waters (Giger et al., 2006, Kiss and Fries, 2009, Loos et al., 2009), drinking waters (Janna et al., 2011), and recycled water for indirect potable reuse (Loi et al., 2013) in concentrations that range from low ng L⁻¹ in natural waters to up to 100 µg L⁻¹ in wastewaters (Giger et al., 2006). In a European survey of polar organic pollutants in municipal wastewaters (8 wastewater treatment plants in 4 countries), BTs and BTHs have been identified among the 4 chemical classes occurring at the highest concentrations (Reemtsma et al., 2006).

To date, there is a lack of toxicity data for BTs and BTHs and assessment of effects on aquatic organisms and human health is a subject of ongoing research. However, acute and chronic toxicity to aquatic organisms has been demonstrated for selected BTs (Cancilla et al., 2003a, Pillard et al., 2001, Seeland et al., 2012), and it has been suggested that 1*H*-benzotriazole (BT)

94 may be an endocrine disrupting compound (Kadar et al., 2010). To reduce exposure and a
95 potential risk for aquatic organisms and human health posed by BTs and BTHs, water treatment
96 processes for their efficient abatement are needed. In the context of this study we consider UV-
97 based processes, which have long been applied for the removal of organic contaminants (Legrini
98 et al., 1993), especially with UV light from low- and medium-pressure mercury lamps.
99 Ultraviolet photolysis in combination with H₂O₂ has also been successfully applied in full-scale
100 water treatment plants (Kruithof et al., 2007), and provides efficient removal for a large variety of
101 organic water contaminants (Baeza and Knappe, 2011, Hofman-Caris et al., 2012, Wols et al.,
102 2013). Treatment with UV light (specifically its UV-C component, spanning a wavelength range
103 of 200–280 nm) exploits the ability of compounds to absorb light and subsequently undergo
104 direct phototransformation leading to their degradation. Owing to the great variability in molar
105 absorption coefficients and reaction quantum yields, a limited number of compounds can be
106 satisfactorily removed by this treatment, *N*-nitrosodimethylamine (NDMA) being a prominent
107 example (Sharpless and Linden, 2003). The advanced oxidation process (AOP) UV/H₂O₂ takes
108 advantage of the production of the hydroxyl radical, which is a highly oxidizing species that
109 reacts efficiently and unselectively with most organic contaminants. During the application of
110 UV/H₂O₂, organic contaminants may be degraded simultaneously by reaction with the hydroxyl
111 radical generated from H₂O₂ photolysis and by direct and indirect phototransformation processes.
112 Indirect phototransformation usually plays a secondary role and is induced through absorption of
113 UV light by water matrix components such as dissolved organic matter (DOM), nitrate or nitrite.
114 Various studies have been devoted to the abatement of BTs and BTHs by AOPs, including UV-
115 based AOPs. Among the BTs, the best studied compound appears to be 1*H*-benzotriazole (BT),
116 which degrades rather slowly under UV-C irradiation, exhibiting a degradation rate which

decreases with increasing pH (Andreozzi et al., 1998, Hem et al., 2003, Liu et al., 2011). The reactivity of BT with the hydroxyl radical was quantified (Karpel Vel Leitner and Roshani, 2010, Naik and Moorthy, 1995) and found to be high, as expected for aromatic compounds. An interesting compilation of data available on BTHs has been provided in a recent review (Antonopoulou et al., 2014). Three representatives of this class of compounds, namely benzothiazole (BTH), 2-mercaptobenzothiazole (2-MBTH) and 2-hydroxybenzothiazole (2-OHBTH) were found to undergo efficient degradation under UV/H₂O₂, as a consequence of their high reactivity with the hydroxyl radical (Andreozzi et al., 2001). However, the great majority of these studies have been performed using contaminant concentrations that are much higher than the concentration ranges found in real waters. In addition, many studies have been performed using pure aqueous solutions. These two drawbacks render a transfer of the obtained results to the treatment of real waters quite difficult.

The goal of this study is to provide a complete and consistent set of quantitative data on the degradation of selected BTs and BTHs via UV photolysis and UV/H₂O₂. The photochemical investigations included the determination of quantum yields and photon fluence based rate constants, for low-pressure mercury lamp conditions ($\lambda=254$ nm), for the phototransformation of the six selected compounds over the pH range of 4–12. Second-order rate constants for the reaction of the compounds with hydroxyl radical were determined by competition kinetics at pH 7. The degradation in wastewater effluent and river water, both spiked with 1 μ M of the selected BTs/BTHs, by UV and UV/H₂O₂ were also investigated.

2. Experimental Section

2.1 Chemicals and solutions. 1*H*-benzotriazole (BT; 99%), 5-methyl-1*H*-benzotriazole (5-MeBT; 98%), 5-chloro-1*H*-benzotriazole (5-ClBT; 99%), benzothiazole (BTH; 96%), 2-mercaptobenzothiazole (2-MBTH; 97%), 2-hydroxybenzothiazole (2-OHBTH; 98%), atrazine (98.9%), *p*-chlorobenzoic acid (pCBA; 99%), *p*-nitroanisol (97%) and pyridine (99.8%) were purchased from Sigma-Aldrich (New South Wales, Australia or Zurich, Switzerland). Hydrogen peroxide solution (H₂O₂; 35%), disodium hydrogen phosphate dihydrate (Na₂HPO₄·2H₂O; ≥98.5%) and sodium dihydrogen phosphate monohydrate (NaH₂PO₄·H₂O; ≥99.0%) were from Fluka (Zurich, Switzerland). Methanol (MeOH; ChromHR grade) and acetonitrile (ACN; ChromHR grade) were from Acros Organics (New Jersey, USA). The ultrapure water used for HPLC eluents and laboratory purposes (e.g. standard solutions) was produced by a “Barnstead Nanopure” water purification system (Thermo Scientific).

Stock solutions for individual BTs (1 mM) and BTHs (0.1–1 mM) were prepared in ultrapure water, and for BTHs a small amount of ACN (<1% vol/vol) was generally used as a co-solvent to ensure complete dissolution. However, for advanced oxidation experiments stock solutions of BTHs were prepared in ultrapure water to avoid any hydroxyl radical scavenging by co-solvents. Since the BTHs did not completely dissolve in ultrapure water due to their limited solubility, prepared stock solutions were filtered and the concentration of the BTHs in the stock solutions were determined by calibration against the standards prepared with ACN. Phosphate buffer solutions (5 mM) were adjusted with a sodium hydroxide solution (NaOH; 160 g L⁻¹) and/or phosphoric acid (H₃PO₄; 85%) when required to obtain the desired pH value (4–12). The pH of all solutions and water samples was monitored by a Metrohm 632 pH-meter with a ThermoScientific Ross Ultra Orion 8115SC pH electrode (Hügli-labortec AG, Switzerland).

Stock solutions of H₂O₂ (50 mM), pCBA (40 µM) and atrazine (20 µM) were prepared in ultrapure water. All solutions were stored at room temperature, except for H₂O₂ and pCBA solutions, which were stored at 4 °C.

River water samples were collected from the Thur River (a tributary of the Rhine River located in North-Eastern Switzerland) and secondary wastewater samples were taken from the Eawag wastewater pilot plant, which receives raw wastewater of mixed urban and industrial origin from the local wastewater treatment plant of the city of Dübendorf. All river and wastewater samples were filtered via 0.45 µm pre-rinsed cellulose nitrate membranes and stored in glass bottles at 4 °C. Water quality parameters are listed in Table 2.

(Table 2)

2.2 Analytical methods. Chemical analyses of the BTs, BTHs, pCBA and atrazine were performed with a Dionex Ultimate 3000 high performance liquid chromatography (HPLC) system (ThermoScientific, Sunnyvale, CA, USA) using a multiple wavelength diode array absorbance detector. An Eclipse XDB-C18 column (150 mm × 4.6 mm I.D., 5 µm; Agilent, NSW, Australia and Zurich, Switzerland) with an Eclipse XDB-C18 guard column (4 mm × 4 mm I.D., 5 µm) was used for the separation. Detailed HPLC conditions for BTs and BTHs analysis are shown in the Supplementary Information (SI), Table S1. Chromeleon 7.0 or 7.1 software was used to process and quantify all data.

2.3 UV-visible absorption spectroscopy and determination of acid dissociation constants. A UVikon940 spectrophotometer (Kontron Instruments) was used to obtain absorption spectra in the wavelength range of 200–700 nm for all the BTs and BTHs at different pH-values (pH 4–12). The pK_a (= -logK_a) of a target compound can be determined by multiple linear regression of

several absorption spectra over a defined wavelength range at different pH values (detailed description of pK_a determination in Text S1, SI).

2.4 Irradiation experiments. Irradiation experiments were performed in glass-stoppered quartz tubes (external diameter 18 mm, internal diameter 15 mm) using a merry-go-round photoreactor (MGRR) (DEMA 125, Hans Mangels GmbH, Bornheim-Roisdorf, Germany). The respective lamp is centered in the photoreactor surrounded by a quartz cooling jacket containing deionized water kept at 25.0 ± 0.2 °C, wherein the sample tubes are placed: a detailed description of the set-up was reported in Wegelin et al. (1994) and Canonica et al. (1995). The kinetic studies of degradation induced by UV-C light and UV/H₂O₂ AOP employed a low-pressure mercury lamp (LP Hg) Heraeus Noblelight model TNN 15/32 (nominal power 15 W), emitting essentially monochromatic light at 254 nm. Determination of the reactivity of the hydroxyl radical with the studied BTs and BTHs was conducted using a Heraeus Noblelight model TQ 718 medium-pressure mercury (MP Hg) lamp and a UVW-55 glass band-pass filter in the cooling jacket as described elsewhere (Huber et al., 2003).

Experimental solutions contained 1 μ M of a single BT or BTH and, for the UV/H₂O₂ experiments, 1 μ M of pCBA to quantify hydroxyl radical concentration. For experiments undertaken to obtain measurements of quantum yields for direct phototransformation and rate constants for hydroxyl radical reactions, the aqueous solutions to be irradiated were buffered with 5 mM phosphate buffer. No pH change was detected after irradiation. Filtered (0.45 μ m) river water and wastewater samples were not otherwise treated prior to advanced oxidation experiments. The addition of the stock solutions (of BTs or BTHs, pCBA and H₂O₂) to the real water samples did not cause any substantial dilution (<2%) of the water matrix components. During irradiation experiments, 400 μ L of solution were withdrawn from each tube at six equidistant time intervals.

Pseudo-first-order phototransformation rate constants, k_{TC}^{obs} (s^{-1}), for a given target compound (TC) were obtained by linear regression of its natural logarithmic relative residual concentration over irradiation time t , according to the following relationship:

$$\ln\left(\frac{[TC]_t}{[TC]_0}\right) = -k_{TC}^{obs}t. \quad (1)$$

To determine the reactivity of BTs and BTHs with the hydroxyl radical, competition kinetics experiments were carried out. A TC (a BT or BTH, 1 μM) and pCBA (reference compound, 1 μM), were irradiated in ultrapure water buffered at pH 7.0 according to the procedure described in Huber et al. (2003). As a photochemical hydroxyl radical source, 5.0 mM hydrogen peroxide was spiked into each MGRR tube. All experiments were conducted in triplicate. The second-order rate constant for the reaction of a TC with the hydroxyl radical, $k_{OH,TC}$, was calculated by equation 2.

$$\ln\left(\frac{[TC]_t}{[TC]_0}\right) = \ln\left(\frac{[pCBA]_t}{[pCBA]_0}\right) \times \frac{k_{OH,TC}}{k_{OH,pCBA}}. \quad (2)$$

Linear regression of $\ln\left(\frac{[TC]_t}{[TC]_0}\right)$ vs. $\ln\left(\frac{[pCBA]_t}{[pCBA]_0}\right)$ yielded the ratio of the rate constants as the line slope, from which $k_{OH,TC}$ was obtained using $k_{OH,pCBA} = 5.0 \times 10^9 M^{-1}s^{-1}$ (Buxton et al., 1988). For advanced oxidation experiments H_2O_2 was added to yield a final concentration of 5.0 $mg L^{-1}$ (147 μM) in the solutions to be irradiated. Assuming hydroxyl radical formation pathways other than from the photolysis of added hydrogen peroxide to be negligible, the steady-state concentration of the hydroxyl radical, $[OH]_{ss}$, was determined using 1 μM pCBA, which was spiked to the river water or wastewater samples as a probe compound. To account for direct

photolysis and other transformation pathways of pCBA not amenable to hydrogen peroxide photolysis, the pseudo-first-order transformation rate constants of pCBA in the presence and absence of hydrogen peroxide, $k_{pCBA}^{obs}(UV/H_2O_2)$ and $k_{pCBA}^{obs}(UV)$, respectively (both determined according to eq. 1), were employed to calculate $[\cdot OH]_{ss}$ by equation 3.

$$[\cdot OH]_{ss} = \frac{k_{pCBA}^{obs}(UV/H_2O_2) - k_{pCBA}^{obs}(UV)}{k_{OH,pCBA}}. \quad (3)$$

The photon fluence rate under LP Hg lamp irradiation was determined daily by chemical actinometry according to Canonica et al. (2008) using aqueous atrazine (5 μM solution buffered at pH = 7 with 5 mM phosphate buffer), with a quantum yield of 0.046 mol einstein⁻¹ (Hessler et al., 1993) and a molar absorption coefficient of 3860 M⁻¹ cm⁻¹ at 254 nm (Nick et al., 1992). Photon fluence rate values were in the range of 10–16 μ einsein m⁻² s⁻¹ for the direct photolysis experiments, and 67–84 μ einsein m⁻² s⁻¹ for the AOP series of experiments. These photon fluence rate values differ due to the use of an old and a new lamp, respectively, for these two experimental series. The concentration of any BT or BTH in solutions amended with H₂O₂ were stable outside of the photoreactor, except for 2-MBTH, for which reductions of 8% and 12% were observed within 60 min at room temperature and in the dark for the river water and the wastewater samples, respectively. The corresponding rate constants were corrected for this thermal reaction.

3. Results and Discussion

3.1 Electronic absorption spectra and dissociation constants. Considering that most of the selected BTs and BTHs exhibit pH-dependent acid-base speciation, electronic absorption spectra of these compounds were measured in the pH range of 4–12 (Figures S1–S6, SI). The

deprotonated species of all BTs (pH=12) exhibit a first absorption band with a maximum at wavelengths between 273 and 280 nm. Upon protonation, the band broadens and shows two maxima or a maximum and a shoulder, with the low-energy feature located approximately at the same wavelength as the maximum of the deprotonated species and the second feature appearing at shorter wavelengths (255–265 nm). A second, stronger absorption band with a maximum at <210 nm for the deprotonated species shifts to lower wavelengths (outside of the experimental wavelength range) upon protonation. Absorption characteristics among BTHs were more diverse. BTH, which does not undergo deprotonation in the studied pH range, had three bands in its pH-independent absorption spectrum, with maxima lying at 284, 251 and <220 nm, respectively. The spectrum of 2-MBTH exhibited two main bands, with maxima at 309 and 233 nm, respectively, for the deprotonated species. These maxima shifted to 321 and 230 nm, respectively, upon protonation. The spectrum of the neutral form of 2-OHBTH (low pH) is similar to that of BTH, with the maxima of the three bands at 286, 242 and <220 nm, respectively. All three bands exhibited a red-shift upon deprotonation, with maxima for the deprotonated form at 295, 258 and \approx 223 nm, respectively.

Except for BTH, the absorption spectra of all selected BTs and BTHs exhibit a remarkable pH dependence, which can be exploited to determine the pK_a of these compounds (for a detailed description of the methodology, see Text S1, SI). The pK_a values determined in this study are reported in Table 1, and compared with previously reported values. For BT, 5-MeBT and 2-OHBTH there is a good agreement with literature. However, for 5-ClBT, the determined pK_a value of 7.7 is significantly lower than a previous value (8.5) reported by Hart et al. (2004). The value determined in the present study is consistent with a reduction of pK_a upon substitution of the aromatic ring with an electron-withdrawing chloro substituent, according to Hammett theory

(Hansch et al., 1991). The pK_a of 2-MBTH was determined to be 7.1, which corresponds to the average of the literature values.

In the context of the present study, the molar absorption coefficient for the wavelength of 254 nm (ϵ_{254nm}^{app}) is of utmost importance for the quantification of phototransformation rates and quantum yields. The pH dependence of ϵ_{254nm}^{app} for both BTs and BTHs, which is the result of the described band shifts in the electronic absorption spectra, is illustrated in Figures 1 (b, d, f) and 2 (b, d, f), respectively. For all BTs, ϵ_{254nm}^{app} decreases with increasing pH by a factor of <1.8 , while 2-MBTH and 2-OHBTH show an increase in ϵ_{254nm}^{app} with pH by a factor of <2.2 . As already pointed out, the absorption coefficient for BTH is independent of pH.

(Figure 1)

(Figure 2)

3.2 Direct phototransformation kinetics. As described in Section 2.4, the decrease in TC concentration as a function of irradiation time during UV-C treatment could be described by first-order kinetics, enabling calculation of pseudo-first-order phototransformation rate constants for all selected BTs and BTHs. Such rate constants depend on irradiation intensity, which typically varies during a series of irradiation experiments. To avoid dependence on experimental conditions and allow comparison with other studies, the results of phototransformation kinetic experiments are given here as apparent photon fluence-based rate constants (see also Canonica et al. (2008)), defined as:

$$k_{E_p^0}^{dp,app} = \frac{k^{dp,app}}{E_p^0}, \quad (4)$$

where the superscript “dp” denotes “direct phototransformation” and the superscript “app” indicates that the rate constant may contain the contribution of more than one species of the TC, E_p^0 (einstein m⁻² s⁻¹) is the photon fluence rate, determined by chemical actinometry. The determined $k_{E_p^0}^{dp,app}$ for BTs and BTHs in the pH range of 4 to 12 are illustrated in Figures 1 and 2, respectively, together with the aforementioned $\varepsilon_{254nm}^{app}$ and the direct phototransformation quantum yields $\Phi_{254nm}^{dp,app}$, which were calculated using the following equation:

$$\Phi_{254nm}^{dp,app} = \frac{k_{E_p^0}^{dp,app}}{2.303\varepsilon_{254nm}^{app}} \quad (5)$$

There is a common trend in the direct phototransformation kinetics of BT, 5-MeBT, 5-ClBT and 2-OHBTH, characterized by a decrease of $k_{E_p^0}^{dp,app}$ with increasing pH and an inflection point that corresponds to the pK_a of each compound (see the speciation curves in Figures 1 and 2). This means that the molecular form of these compounds, which dominates at pH below the pK_a, is more photoreactive than the deprotonated form. The quantum yields follow the same trend, except for 5-ClBT, which exhibits a slightly higher quantum yield above the pK_a. In contrast, 2-MBTH follows an inverse trend with respect to these three compounds, since $k_{E_p^0}^{dp,app}$ markedly increases with increasing pH. For BTH, which does not exhibit a pK_a in the studied pH range, $k_{E_p^0}^{dp,app}$, $\varepsilon_{254nm}^{app}$ and $\Phi_{254nm}^{dp,app}$ are constant.

For a quantitative analysis of the pH dependence of the various photochemical parameters we applied a model which assumes a constant phototransformation quantum yield for each acid-base species of the TC under consideration. For the mathematical treatment we refer to a previous

study (Canonica et al., 2008). Briefly, $k_{E_p^0}^{dp,app}$ and $\varepsilon_{254nm}^{app}$ were fitted separately to equations 6 and 7, respectively:

$$k_{E_p^0}^{dp,app} = k_{E_p^0,1}^{dp} + (k_{E_p^0,2}^{dp} - k_{E_p^0,1}^{dp})\alpha_2 , \quad (6)$$

$$\varepsilon_{254nm}^{app} = \varepsilon_{254nm,1} + (\varepsilon_{254nm,2} - \varepsilon_{254nm,1})\alpha_2 , \quad (7)$$

with the fitting parameters $k_{E_p^0,1}^{dp}$ and $k_{E_p^0,2}^{dp}$ the photon fluence-based direct phototransformation rate constants for the molecular and deprotonated form of the TC, respectively, and the fitting parameters $\varepsilon_{254nm,1}$ and $\varepsilon_{254nm,2}$ defined analogously. The fraction of deprotonated form present at a given pH (α_2) is calculated using equation 8.

$$\alpha_2 = \frac{1}{1 + 10^{pK_a - pH}} . \quad (8)$$

After these fit parameters had been determined, the quantum yields for the molecular ($i=1$) and deprotonated species ($i=2$) were determined using equation 9.

$$\Phi_{254nm,i}^{dp} = \frac{k_{E_p^0,i}^{dp}}{2.303\varepsilon_{254nm,i}} . \quad (9)$$

All best-fit parameters are presented in Table 3, while the dashed lines in Figure 1 and 2 represent the best-fit functions. Fits of $k_{E_p^0}^{dp,app}$ data to equation 6 are satisfactory, supporting the validity of the model. The quantum yields values obtained for BT, 0.016 ± 0.002 and 0.0026 ± 0.0005 mol einstein⁻¹ for the molecular and deprotonated form, respectively, compare fairly well with the corresponding values of 0.0239 and 0.00215, obtained at the pH values of 3.0 and 11.0, respectively, in a photolysis study (Andreozzi et al., 1998). Quantum yields from another study (Benitez et al., 2013) follow the same speciation trend but are higher (by a factor of ≈ 2 at low pH and by a factor of ≈ 4 at high pH) than in this and the aforementioned study. For 2-

MBTH, data above pH 8 is consistent with the deprotonated form exhibiting a constant quantum yield, and the calculated value of $\Phi_{254nm,2}^{dp}$ (0.028 ± 0.014 mol einstein⁻¹) is comparable to 0.02, the value determined in a previous study at the wavelength of 313 nm (Malouki et al., 2004). However at low pH the quantum yield continues to decrease with decreasing pH, indicating that $\Phi_{254nm,1}^{dp}$ is pH-dependent. Such a pH dependence might result from the acid-base speciation of excited-state species or from acid-catalyzed deactivation of phototransformation intermediates.

(Table 3)

3.3 Reactivity of benzotriazoles and benzothiazoles with the hydroxyl radical. Second-order rate constants for the reaction of TCs with the hydroxyl radical are listed in Table 4. The constants for the BTs determined in this study are in the range of $8.3\text{--}10.8 \times 10^9 \text{ M}^{-1} \text{ s}^{-1}$, which is typical for aromatic compounds (Buxton et al., 1988, Haag and Yao, 1992, Huber et al., 2003). For BT, the rate constant is in satisfactory agreement with literature values. The constant for BTH is in the same range as for the BTs, while 2-OHBTH exhibits the lowest reactivity among all investigated TCs ($\approx 5.1 \times 10^9 \text{ M}^{-1} \text{ s}^{-1}$). Both are somewhat higher than available literature data (Table 4). No second-order reaction rate constant could be determined for 2-MBTH due to its fast direct phototransformation under the employed irradiation conditions. Overall, the results indicate a high reactivity of the BTs and BTHs with the hydroxyl radical, suggesting that AOPs could be effective tools to abate these compounds from drinking water and wastewater.

(Table 4)

3.4 Removal of benzotriazoles and benzothiazoles by the UV/H₂O₂ process. The AOP UV/H₂O₂ was applied to treat river water and wastewater samples spiked with a low concentration (1 µM) of a single BT or BTH. The removal of the TCs under UV/H₂O₂ was always faster than under UV irradiation alone, and followed pseudo-first-order kinetics (Figures S7 and S8, SI). The corresponding pseudo-first-order transformation rate constants according to equation 1 were converted to photon fluence-based rate constants, $k_{E_p^0}^{AOP}$ (transformation by the UV/H₂O₂ process) and $k_{E_p^0}^{UV}$ (transformation by UV alone, without addition of H₂O₂, in river water and wastewater samples), analogously to the direct phototransformation rate constants (equation 4). Photon fluence rates determined by actinometry were corrected with a light screening factor (0.973 for river water and 0.925 for wastewater calculated according to Wenk and Canonica (2012) to consider the fact that UV-C light is partially absorbed by water matrix components, mainly by dissolved organic matter. The photon fluence-based rate constants are compiled in Table 5. For all TCs $k_{E_p^0}^{AOP}$ values are significantly higher (3–9 times) than $k_{E_p^0}^{UV}$ values, clearly implying that the reaction with hydroxyl radicals formed by photolysis of H₂O₂ dominates the removal of all TCs in the selected waters and at the employed H₂O₂ concentration (see $k_{E_p^0}^{AOP} - k_{E_p^0}^{UV}$ and the percentage values in Table 5). For each BT and BTH, the $k_{E_p^0}^{AOP}$ values for river water are consistently higher than those for wastewater, which may be ascribed to the higher hydroxyl radical scavenging rate of the wastewater. Neglecting hydroxyl radical formation under UV alone, which may occur from photoactive precursors such as nitrate and/or nitrite, and DOM/EfOM, the following equations hold for the UV/H₂O₂-induced degradation for a given TC:

$$k_{E_p^0}^{AOP}(TC) = k_{E_p^0}^{UV}(TC) + k_{OH,TC} \frac{[OH]_{ss}}{E_p^0}, \quad (10)$$

$$k_{E_p^0}^{AOP}(TC) - k_{E_p^0}^{UV}(TC) = k_{OH,TC} \frac{[OH]_{ss}}{E_p^0} \quad (11)$$

A comparison of the rate constants for the hydroxyl radical-induced reaction, $k_{E_p^0}^{AOP} - k_{E_p^0}^{UV}$, for the seven compounds listed in Table 5 yields, on average, a 35% higher value for river water than for wastewater. Since the AOP experiments were run with the addition of pCBA as a reference compound for the hydroxyl radical reaction (see last line in Table 5), equation 11, after transformation to equation 12, provides an alternative method to estimate the second-order rate constant for the reaction of a TC with the hydroxyl radical.

$$k_{OH,TC} = \frac{k_{E_p^0}^{AOP}(TC) - k_{E_p^0}^{UV}(TC)}{k_{E_p^0}^{AOP}(pCBA) - k_{E_p^0}^{UV}(pCBA)} k_{OH,pCBA} \quad (12)$$

Application of equation 12 to the data in Table 5 provides the $k_{OH,TC}$ values listed in Table S2, SI. Compared to values determined by competition kinetics in buffered pure water (Table 4), $k_{OH,TC}$ values in river water or wastewater are between 15 and 42% lower for BTH and the three selected BTs, and 22% higher for 2-OHBTH. These deviations might arise from side-reactions occurring in the very complex chemical system represented by the real waters treated with UV/H₂O₂. The value for 2-MBTH, for which a direct comparison cannot be made because of the missing competition kinetics value, appears to be unrealistically high, and exceeds the literature value from Andreozzi et al. (2001) by a factor of 6. In view of the observed reaction of 2-MBTH with H₂O₂ in the dark (see Section 2.4), the reaction of photoexcited 2-MBTH with H₂O₂, leading to an increased quantum yield of direct phototransformation, seems to be a plausible explanation for this enhanced reactivity. Alternatively, the carbonate radical formed by the reaction of the hydroxyl radical with bicarbonate and carbonate present in the real waters (Canonica et al., 2005) could also contribute to the acceleration of 2-MBTH transformation.

The UV reactivity of the target compounds in the absence of H_2O_2 was also considered by comparing $k_{E_p^0}^{UV}$ (Table 5) with direct phototransformation rate constants calculated for the pH in the real waters (see Table S3, SI). For the BTs, except for a few lower values measured in the real waters, the calculated direct phototransformation constants reproduce the $k_{E_p^0}^{UV}$ values relatively well, which indicates the water matrix had a limited effect on phototransformation reactions. In contrast, for the BTHs the $k_{E_p^0}^{UV}$ values are significantly higher than calculated direct phototransformation values, which is probably due to indirect phototransformation reactions or the enhancement of direct phototransformation by the water matrix. However, in the context of the AOP treatment these effects of UV radiation alone are of limited importance, since the transformation of all studied BTs and BTHs is dominated by the reaction with the hydroxyl radical (see %-values in Table 5).

(Table 5)

3.5 Assessment of the energy requirement for abatement of BTs and BTHs by UV and UV/ H_2O_2 .

As the UV and UV/ H_2O_2 processes are just two possible options among many other water purification methods, one important aspect to consider for full-scale implementation is the energy consumption (and indirectly the costs) of these processes. To calculate energy consumption, we use $H_{r,90\%}$, the fluence required to remove 90% of each TC at zero optical density as the target end-point. This end-point is consistent with another recent study (Katsoyiannis et al., 2011) and the IUPAC recommendations for assessment of AOP figures-of-merit when TC concentrations are low (Bolton et al., 2001). The value of $H_{r,90\%}$ is compound-specific and depends on the extent

of hydroxyl radical scavenging by the water matrix. It can be calculated from the photon fluence-based rate constants given in Table 5, $k_{E_p^0}^{AOP}$ (transformation by the UV/H₂O₂ process) and $k_{E_p^0}^{UV}$ (transformation by solely UV treatment), using eq. 13.

$$H_{r,90\%}^0 = \frac{2.303}{k_{E_p^0}^{AOP}} \times (4.71 \times 10^5 \text{ J einstein}^{-1}), \quad (13)$$

where the term in parentheses is the appropriate photon-to-energy conversion factor for $\lambda=254$ nm, and $k_{E_p^0}^{AOP}$ is replaced with $k_{E_p^0}^{UV}$ for the corresponding calculations for transformation by UV treatment. The $H_{r,90\%}$ values in Figure 3 show that the fluence required for a 90% abatement of BTs and BTHs with treatment using UV light alone are up to 7 times higher compared to UV/H₂O₂ treatment. Compared to all other BTs and BTHs, 2-MBTH needs a much lower $H_{r,90\%}$ because of its much higher reactivity (see Section 3.4). The $H_{r,90\%}$ values calculated for UV/H₂O₂ treatment are up to 100 times higher than the conventional UV doses used for drinking water disinfection (German and Austrian legislation prescribes a UV dose of 400 J m⁻²), but they are typical for the removal of organic micropollutants in the production of drinking water (Kruithof et al., 2002, Kruithof et al., 2007).

(Figure 3)

The energy consumption for micropollutant removal by UV/H₂O₂ treatment depends on several factors including the reactor design (path length, lamp), the applied concentration of H₂O₂ (energy for H₂O₂ production), the properties of water matrix, in particular its hydroxyl radical scavenging capacity, and the chemical properties of the target micropollutants (Katsoyiannis et al., 2011). To simplify the assessment of energy consumption, calculations are made for a limited

selection of cases considered in a previous study (Katsoyiannis et al., 2011), using pCBA as a reference compound because its fluence-based rate constants (Table 5) are comparable to all BTs and BTHs except for 2-MBTH. For an optical path length of 5 cm, a 90% removal of BTs and BTHs would be achieved with an energy of 0.23 kWh m⁻³ for a surface water with 1.3 mg C L⁻¹ and with 0.82 kWh m⁻³ for a wastewater with 3.9 mg C L⁻¹. In an alternative approach, the energy consumption calculations according to Katsoyiannis et al. were applied to the present data for BTH, which requires the highest treatment energy among the studied BTs and BTHs. For a 5 cm optical path length in a hypothetical photoreactor and an added H₂O₂ concentration of 5 mg L⁻¹, energy values of 0.59 and 1.02 kWh m⁻³ were calculated for the treatment of river water and wastewater, respectively. These energy consumption values are in the same range as the requirement of 0.54 kWh m⁻³ evaluated for a drinking water plant operated with UV/H₂O₂ treatment (6 mg L⁻¹ of H₂O₂) to achieve >60% degradation of various organic pollutants (Kruithof and Martijn, 2013). The higher reactivity of 2-MBTH compared to the other studied compounds reduces the energy consumption by a factor of ≈4.

4. Conclusions

- All studied benzotriazoles (BTs) and benzothiazoles (BTHs) studied are photoreactive under UV-C light ($\lambda=254$ nm) and exhibit (except for BTH) pH-dependent direct phototransformation rates in the pH range of 4–12, in accordance to their deprotonation equilibria (pK_a values in the range of 7.1–8.8). For all BTs and 2-hydroxybenzothiazole, the molecular form is more photoreactive than the corresponding deprotonated form, while 2-mercaptobenzothiazole exhibits the reverse behavior.

- Direct phototransformation quantum yields were found to vary from $\approx 1 \times 10^{-3}$ to $\approx 3 \times 10^{-2}$ mol einstein⁻¹, which renders the degradation of BTs and BTHs by UV treatment without additives quite inefficient.
- The reactivities of BTs and BTHs with the hydroxyl radical were determined to be high, with second-order rate constants in the range of $5.1\text{--}10.8 \times 10^9 \text{ M}^{-1} \text{ s}^{-1}$.
- The application of the AOP UV/H₂O₂ to the treatment of a river water and a wastewater demonstrated an efficient removal for both contaminant classes (BTs, BTHs).
- BTs and BTHs in waters treated with UV/H₂O₂ are mainly transformed by reaction with the hydroxyl radical.

Acknowledgements

This work was supported by the Swiss National Science Foundation in the frame of the *National research programme "Sustainable Water Management" (NRP 61)*, Project No. 406140-125856. Clara Loi's research visit to Eawag was financially supported by the Australian Government (Australian Postgraduate Award and Australian Research Council Linkage project LP0989326), Curtin University (Curtin Research Scholarship) and Water Research Australia (WaterRA PhD Scholarship). The authors thank Hans-Ulrich Laubscher for technical support.

Appendix A. Supplementary data

Supplementary data related to this article can be found at

References

- Andreozzi, R., Caprio, V., Insola, A., Longo, G., 1998. Photochemical degradation of benzotriazole in aqueous solution. *Journal of Chemical Technology and Biotechnology* 73(2), 93-98.
- Andreozzi, R., Caprio, V., Marotta, R., 2001. Oxidation of benzothiazole, 2-mercaptobenzothiazole and 2-hydroxybenzothiazole in aqueous solution by means of H_2O_2 /UV or photoassisted Fenton systems. *Journal of Chemical Technology and Biotechnology* 76(2), 196-202.
- Antonopoulou, M., Evgenidou, E., Lambropoulou, D., Konstantinou, I., 2014. A review on advanced oxidation processes for the removal of taste and odor compounds from aqueous media. *Water Research* 53, 215-234.
- Baeza, C., Knappe, D.R.U., 2011. Transformation kinetics of biochemically active compounds in low-pressure UV photolysis and UV/ H_2O_2 advanced oxidation processes. *Water Research* 45(15), 4531-4543.
- Benitez, F.J., Acero, J.L., Real, F.J., Roldan, G., Rodriguez, E., 2013. Photolysis of model emerging contaminants in ultra-pure water: Kinetics, by-products formation and degradation pathways. *Water Research* 47(2), 870-880.
- Bolton, J.R., Bircher, K.G., Tumas, W., Tolman, C.A., 2001. Figures-of-merit for the technical development and application of advanced oxidation technologies for both electric- and solar-driven systems - (IUPAC Technical Report). *Pure and Applied Chemistry* 73(4), 627-637.
- Brownlee, B.G., Carey, J.H., Macinnis, G.A., Pellizzari, I.T., 1992. Aquatic environmental chemistry of 2-(thiocyanomethylthio)benzothiazole and related benzothiazoles. *Environmental Toxicology and Chemistry* 11(8), 1153-1168.
- Bugby, A., Parbery, C., Sykes, R.L., Taylor, C.D., 1990. Analysis of biological-control materials encountered in leather production. *Journal of the Society of Leather Technologists and Chemists* 74(5), 134-141.
- Buxton, G.V., Greenstock, C.L., Helman, W.P., Ross, A.B., 1988. Critical review of rate constants for reactions of hydrated electrons, hydrogen atoms and hydroxyl radicals ($\cdot\text{OH}/\cdot\text{O}^-$) in aqueous solution. *Journal of Physical and Chemical Reference Data* 17(2), 513-886.
- Cancilla, D.A., Martinez, J., Van Aggelen, G.C., 1998. Detection of aircraft deicing/antiicing fluid additives in a perched water monitoring well at an international airport. *Environmental Science & Technology* 32(23), 3834-3835.

522 Cancilla, D.A., Baird, J.C., Geis, S.W., Corsi, S.R., 2003a. Studies of the environmental fate and
 523 effect of aircraft deicing fluids: Detection of 5-methyl-1*H*-benzotriazole in the fathead minnow
 524 (*Pimephales promelas*). *Environmental Toxicology and Chemistry* 22(1), 134-140.

525 Cancilla, D.A., Baird, J.C., Rosa, R., 2003b. Detection of aircraft deicing additives in
 526 groundwater and soil samples from Fairchild Air Force Base, a small to moderate user of deicing
 527 fluids. *Bulletin of Environmental Contamination and Toxicology* 70(5), 868-875.

528 Canonica, S., Jans, U., Stemmler, K., Hoigné, J., 1995. Transformation kinetics of phenols in
 529 water: Photosensitization by dissolved natural organic material and aromatic ketones.
 530 *Environmental Science & Technology* 29(7), 1822-1831.

531 Canonica, S., Kohn, T., Mac, M., Real, F.J., Wirz, J., Von Gunten, U., 2005. Photosensitizer
 532 method to determine rate constants for the reaction of carbonate radical with organic compounds.
 533 *Environmental Science & Technology* 39(23), 9182-9188.

534 Canonica, S., Meunier, L., Von Gunten, U., 2008. Phototransformation of selected
 535 pharmaceuticals during UV treatment of drinking water. *Water Research* 42(1-2), 121-128.

536 De Orsi, D., Giannini, G., Gagliardi, L., Porra, R., Berri, S., Bolasco, A., Carpani, I., Tonelli, D.,
 537 2006. Simple extraction and HPLC determination of UV-A and UV-B filters in sunscreen
 538 products. *Chromatographia* 64(9-10), 509-515.

539 Engels H.-W., W., H.-J., Abele M., Pieroth M. and Hofmann W., 1993. *Ullmann's Encyclopedia*
 540 *of Industrial Chemistry* VCH Weinheim.

541 Fries, E., Gocht, T., Klasmeier, J., 2011. Occurrence and distribution of benzothiazole in the
 542 Schwarzbach watershed (Germany). *Journal of Environmental Monitoring* 13(10), 2838-2843.

543 Giger, W., Schaffner, C., Kohler, H.P.E., 2006. Benzotriazole and tolyltriazole as aquatic
 544 contaminants. 1. Input and occurrence in rivers and lakes. *Environmental Science & Technology*
 545 40(23), 7186-7192.

546 Haag, W.R., Yao, C.C.D., 1992. Rate constants for reaction of hydroxyl radicals with several
 547 drinking water contaminants. *Environmental Science & Technology* 26(5), 1005-1013.

548 Hansch, C., Leo, A., Taft, R.W., 1991. A survey of hammett substituent constants and resonance
 549 and field parameters. *Chemical Reviews* 91(2), 165-195.

550 Hart, D.S., Davis, L.C., Erickson, L.E., Callender, T.M., 2004. Sorption and partitioning
 551 parameters of benzotriazole compounds. *Microchemical Journal* 77(1), 9-17.

552 Hartley, D., Kidd, H., 1987. *The Agrochemical Handbook* The Royal Society of Chemistry
 553 Nottingham.

554 Hem, L.J., Hartnik, T., Roeth, R., Breedveld, G.D., 2003. Photochemical degradation of
 555 benzotriazole. *Journal of Environmental Science and Health Part a-Toxic/Hazardous Substances*
 556 *& Environmental Engineering* 38(3), 471-481.

557 Hessler, D.P., Gorenflo, V., Frimmel, F.H., 1993. Degradation of aqueous atrazine and
 558 metazachlor solutions by UV and UV/H₂O₂ - Influence of pH and herbicide concentration. *Acta*
 559 *Hydrochimica et Hydrobiologica* 21(4), 209-214.

560 Hofman-Caris, C.H.M., Harmsen, D.J.H., Beerendonk, E.F., Knol, A.H., Metz, D.H., Wols, B.A.,
 561 2012. Prediction of advanced oxidation performance in pilot UV/H₂O₂ reactor systems with MP-
 562 and LP-UV lamps. *Ozone-Science & Engineering* 34(2), 120-124.

563 Huber, M.M., Canonica, S., Park, G.Y., Von Gunten, U., 2003. Oxidation of pharmaceuticals
 564 during ozonation and advanced oxidation processes. *Environmental Science & Technology* 37(5),
 565 1016-1024.

566 Huntscha, S., Singer, H.P., McArdell, C.S., Frank, C.E., Hollender, J., 2012. Multiresidue
 567 analysis of 88 polar organic micropollutants in ground, surface and wastewater using online
 568 mixed-bed multilayer solid-phase extraction coupled to high performance liquid chromatography-
 569 tandem mass spectrometry. *Journal of Chromatography A* 1268, 74-83.

570 Janna, H., Scrimshaw, M.D., Williams, R.J., Churchley, J., Sumpter, J.P., 2011. From dishwasher
 571 to tap? Xenobiotic substances benzotriazole and tolyltriazole in the environment. *Environmental*
 572 *Science & Technology* 45(9), 3858-3864.

573 Kadar, E., Dashfield, S., Hutchinson, T.H., 2010. Developmental toxicity of benzotriazole in the
 574 protochordate *Ciona intestinalis* (Chordata, Ascidiace). *Analytical and Bioanalytical Chemistry*
 575 396(2), 641-647.

576 Karpel Vel Leitner, N., Roshani, B., 2010. Kinetic of benzotriazole oxidation by ozone and
 577 hydroxyl radical. *Water Research* 44(6), 2058-2066.

578 Katsoyiannis, I.A., Canonica, S., von Gunten, U., 2011. Efficiency and energy requirements for
 579 the transformation of organic micropollutants by ozone, O₃/H₂O₂ and UV/H₂O₂. *Water Research*
 580 45(13), 3811-3822.

581 Kennedy, M.J., 1986. High-performance liquid-chromatographic analysis of preservative-treated
 582 timber for 2-(thiocyanomethylthio)benzothiazole and methylene bithiocyanate. *Analyst* 111(6),
 583 701-705.

584 Kiss, A., Fries, E., 2009. Occurrence of benzotriazoles in the rivers Main, Hengstbach, and
 585 Hegbach (Germany). *Environmental Science and Pollution Research* 16(6), 702-710.

586 Klopfer, A., Jekel, M., Reemtsma, T., 2005. Occurrence, sources, and fate of benzothiazoles in
 587 municipal wastewater treatment plants. *Environmental Science & Technology* 39(10), 3792-3798.

588 Kruithof, J.C., Kamp, P.C., Belosevic, M., 2002. UV/H₂O₂-treatment: the ultimate solution for
 589 pesticide control and disinfection. *Water Science and Technology: Water Supply* 2(1), 113-122.

590 Kruithof, J.C., Kamp, P.C., Martijn, B.J., 2007. UV/H₂O₂ treatment: A practical solution for
 591 organic contaminant control and primary disinfection. *Ozone-Science & Engineering* 29(4), 273-
 592 280.

593 Kruithof, J.C., Martijn, B.J., 2013. UV/H₂O₂ treatment: an essential process in a multi barrier
 594 approach against trace chemical contaminants. *Water Science and Technology-Water Supply*
 595 13(1), 130-138.

596 Legrini, O., Oliveros, E., Braun, A.M., 1993. Photochemical processes for water treatment.
 597 *Chemical Reviews* 93(2), 671-698.

598 Liu, Y.S., Ying, G.G., Shareef, A., Kookana, R.S., 2011. Photolysis of benzotriazole and
 599 formation of its polymerised photoproducts in aqueous solutions under UV irradiation.
 600 *Environmental Chemistry* 8(2), 174-181.

Loi, C.H., Buseti, F., Linge, K.L., Joll, C.A., 2013. Development of a solid-phase extraction liquid chromatography tandem mass spectrometry method for benzotriazoles and benzothiazoles in wastewater and recycled water. *Journal of Chromatography A* 1299, 48-57.

Loos, R., Gawlik, B.M., Locoro, G., Rimaviciute, E., Contini, S., Bidoglio, G., 2009. EU-wide survey of polar organic persistent pollutants in European river waters. *Environmental Pollution* 157(2), 561-568.

Malouki, M.A., Richard, C., Zertal, A., 2004. Photolysis of 2-mercaptobenzothiazole in aqueous medium - Laboratory and field experiments. *Journal of Photochemistry and Photobiology A-Chemistry* 167(2-3), 121-126.

Naik, D.B., Moorthy, P.N., 1995. Studies on the transient species formed in the pulse radiolysis of benzotriazole. *Radiation Physics and Chemistry* 46(3), 353-357.

Nick, K., Schöler, H., Mark, G., Söylemez, T., Akhlaq, M.S., Schuchmann, H.-P., von Sonntag, C., 1992. Degradation of some triazine herbicides by UV radiation such as used in the UV disinfection of drinking water *Journal of Water Supply Research and Technology-Aqua* 41(2), 82-87.

Pillard, D.A., Cornell, J.S., Dufresne, D.L., Hernandez, M.T., 2001. Toxicity of benzotriazole and benzotriazole derivatives to three aquatic species. *Water Research* 35(2), 557-560.

Reddy, C.M., Quinn, J.G., 1997. Environmental chemistry of benzothiazoles derived from rubber. *Environmental Science & Technology* 31(10), 2847-2853.

Reemtsma, T., Fiehn, O., Kalnowski, G., Jekel, M., 1995. Microbial transformation and biological effects of fungicide-derived benzothiazoles determined in industrial wastewater. *Environmental Science & Technology* 29(2), 478-485.

Reemtsma, T., Weiss, S., Mueller, J., Petrovic, M., Gonzalez, S., Barcelo, D., Ventura, F., Knepper, T.P., 2006. Polar pollutants entry into the water cycle by municipal wastewater: A European perspective. *Environmental Science & Technology* 40(17), 5451-5458.

Reemtsma, T., Miehe, U., Duennbier, U., Jekel, M., 2010. Polar pollutants in municipal wastewater and the water cycle: Occurrence and removal of benzotriazoles. *Water Research* 44(2), 596-604.

Seeland, A., Oetken, M., Kiss, A., Fries, E., Oehlmann, J., 2012. Acute and chronic toxicity of benzotriazoles to aquatic organisms. *Environmental Science and Pollution Research* 19(5), 1781-1790.

Sharpless, C.M., Linden, K.G., 2003. Experimental and model comparisons of low- and medium-pressure Hg lamps for the direct and H₂O₂ assisted UV photodegradation of *N*-nitrosodimethylamine in simulated drinking water. *Environmental Science & Technology* 37(9), 1933-1940.

Voutsas, D., Hartmann, P., Schaffner, C., Giger, W., 2006. Benzotriazoles, alkylphenols and bisphenol A in municipal wastewaters and in the Glatt River, Switzerland. *Environmental Science and Pollution Research* 13(5), 333-341.

Wegelin, M., Canonica, S., Mechsner, K., Fleischmann, T., Pesaro, F., Metzler, A., 1994. Solar water disinfection: Scope of the process and analysis of radiation experiments. *J. Water Supply Res. Technol. - Aqua* 43(3), 154-169.

642 Weiss, S., Jakobs, J., Reemtsma, T., 2006. Discharge of three benzotriazole corrosion inhibitors
643 with municipal wastewater and improvements by membrane bioreactor treatment and ozonation.
644 Environmental Science & Technology 40(23), 7193-7199.

645 Wenk, J., Canonica, S., 2012. Phenolic antioxidants inhibit the triplet-induced transformation of
646 anilines and sulfonamide antibiotics in aqueous solution. Environmental Science & Technology
647 46(10), 5455-5462.

648 Wik, A., Dave, G., 2009. Occurrence and effects of tire wear particles in the environment - A
649 critical review and an initial risk assessment. Environmental Pollution 157(1), 1-11.

650 Wols, B.A., Hofman-Caris, C.H.M., Harmsen, D.J.H., Beerendonk, E.F., 2013. Degradation of
651 40 selected pharmaceuticals by UV/H₂O₂. Water Research 47(15), 5876-5888.

652

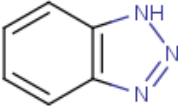
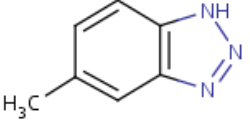
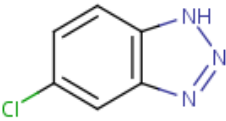
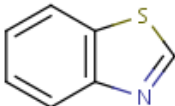
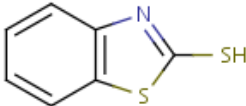
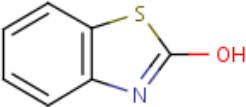
Table 1 – Chemical structure and acid dissociation constants of the selected BTs and BTHs			
Compound	Structure	pK_a^a determined in this study	pK_a reported in other studies
1 <i>H</i> -Benzotriazole (BT)		8.3±0.2	8.62 ^b , 8.27 ^c 8.37 ^d
5-Methyl-1 <i>H</i> -benzotriazole (5-MeBT)		8.5±0.3	8.5 ^e
5-Chloro-1 <i>H</i> -benzotriazole (5-ClBT)		7.7±0.1	8.5 ^e
Benzothiazole (BTH)		<i>n.d.</i> ^f	1.2 ^g
2-Mercaptobenzothiazole (2-MBTH)		7.1±0.1	6.95 ^g , 6.7 ^h , 7.2 ⁱ , 7.69 ^j
2-Hydroxybenzothiazole (2-OHBTH)		8.9±0.3	8.65 ^j
^a Values and standard errors obtained from the linear regression method (Text S1, SI). ^b Andreozzi et al., 1998; ^c Wang et al., 2000; ^d Yang et al., 2011; ^e Hart et al., 2004; ^f not determined, because outside of the studied pH range; ^g Eicher and Hauptmann, 2003; ^h Malouki et al., 2004; ⁱ Brownlee et al., 1992; ^j Andreozzi et al., 2001.			

Table 2 – Water quality parameters of the sampled wastewater and river water							
	DOC (mgC L ⁻¹)	pH	Alkalinity (mmol L ⁻¹)	Nitrate (mgN L ⁻¹)	Nitrite (µgN L ⁻¹)	$a_{254\text{ nm}}$ ^a (cm ⁻¹)	$SUVA_{254\text{ nm}}$ (L mgC ⁻¹ cm ⁻¹)
Wastewater	4.8	7.9	6.4	2.9	4.2	0.0614	0.0128
River water	2.5	8.3	4.9	2.4	9.6	0.0214	0.0086

Notes: ^a Decadic absorption coefficient of the filtered water measured at 254 nm;

^b Specific absorption coefficient: $SUVA_{254\text{ nm}} = a_{254\text{ nm}}/DOC$.

Table 3 – Kinetic parameters for the direct phototransformation of the select benzotriazoles and benzothiazoles ^a

Compound	$k_{E_p^0,1}^{dp}$ ^b (m ² einstein ⁻¹)	$\mathcal{E}_{254nm,1}$ ^b (m ² mol ⁻¹)	$\Phi_{254nm,1}^{dp}$ ^c (mol einstein ⁻¹)	$k_{E_p^0,2}^{dp}$ ^c (m ² einstein ⁻¹)	$\mathcal{E}_{254nm,2}$ ^c (m ² mol ⁻¹)	$\Phi_{254nm,2}^{dp}$ ^c (mol einstein ⁻¹) ^c
BT	22.7 ± 2.5	614 ± 19	0.016 ± 0.002	2.7 ± 0.4	450 ± 59	0.0026 ± 0.0005
5-MeBT	15.9 ± 2.6	523 ± 15	0.013 ± 0.002	3.9 ± 1.1	344 ± 30	0.0049 ± 0.0015
5-ClBT	16.3 ± 1.2	507 ± 3	0.014 ± 0.001	11.2 ± 2.9	293 ± 4	0.017 ± 0.004
BTH	1.2 ± 0.2 ^e	545 ± 28 ^e	0.00096 ± 0.00015 ^f	n.a. ^d	n.a.	n.a.
2-MBTH	9.3 ± 4.5	538 ± 5	0.008 ± 0.004	51 ± 25	803 ± 16	0.028 ± 0.014
2-OHBTH	2.6 ± 0.1	375 ± 1	0.0030 ± 0.0001	0.72 ± 0.05	815 ± 4	0.00038 ± 0.00003

^a All uncertainties represent 95% confidence intervals.
^b Uncertainties calculated by linear regression analysis unless noted otherwise.
^c Uncertainties determined by linear regression analysis and application of the Gaussian error propagation rule unless noted otherwise.
^d n.a.: not applicable.
^e Average/uncertainty of 7 values measured over the pH range of 4–12.
^f Uncertainty calculated by application of the Gaussian error propagation rule.

Table 4 – Second-order rate constants for the reaction of the selected benzotriazoles and benzothiazoles with the hydroxyl radical at pH 7.0		
Target compound (TC)	$k_{OH,TC}$ ($10^9 \text{ M}^{-1} \text{ s}^{-1}$)	
	This study	Literature values
BT	8.34 ± 0.37	14.2 (pH 8.45)^a , 10.7 (pH 6.25)^a ; 9.0 (pH 10.5)^b , 7.6 (pH 5.8)^b
5-MeBT	8.71 ± 0.12	-
5-CIBT	10.77 ± 0.26	-
BTH	8.61 ± 0.23	3.85^c
2-MBTH	n.d. ^d	4.27^c
2-OHBTH	5.08 ± 0.44	3.97^c
^a Karpel Vel Leitner and Roshani, 2010; ^b Naik and Moorthy, 1995; ^c Andreozzi et al., 2001; ^d n.d.: not determined		

Table 5 – Photon fluence-based rate constants ($\text{m}^2 \text{einstein}^{-1}$) of the UV/ H_2O_2 process ($[\text{H}_2\text{O}_2]=5 \text{ mg L}^{-1}$) and the UV treatment for the studied wastewater and river water ^{a, b}

Target compound (TC)	Wastewater			River water		
	$k_{E_p^0}^{AOP}$	$k_{E_p^0}^{UV}$	$k_{E_p^0}^{AOP} - k_{E_p^0}^{UV} \text{ }^c$	$k_{E_p^0}^{AOP}$	$k_{E_p^0}^{UV}$	$k_{E_p^0}^{AOP} - k_{E_p^0}^{UV} \text{ }^c$
BT	41.9 ± 1.7	11.2 ± 1.3	30 (73%)	47.9 ± 1.7	6.5 ± 1.1	41 (87%)
5-MeBT	45.6 ± 1.7	6.2 ± 5.1	39 (86%)	61.2 ± 2.6	9.2 ± 1.5	52 (85%)
5-ClBT	46.6 ± 3.0	13.5 ± 2.6	33 (73%)	58.1 ± 2.6	10.7 ± 1.7	47 (82%)
BTH	29.0 ± 2.5	4.4 ± 2.3	25 (85%)	42.5 ± 5.1	4.7 ± 2.4	38 (89%)
2-MBTH	212.7 ± 6.4	69.8 ± 2.1	143 (67%)	250 ± 8.4	81.9 ± 2.7	169 (67%)
2-OHBTH	41.2 ± 3.3	8.5 ± 5.2	33 (79%)	51.4 ± 7.3	7.1 ± 5.5	44 (86%)
pCBA	36.2 ± 2.1	8.7 ± 1.1	27 (76%)	43.3 ± 1.4	8.6 ± 2.3	35 (80%)

^a Irradiation at 254 nm.

^b The errors indicate 95% confidence intervals obtained from linear regression.

^c Percentage of hydroxyl radical-induced transformation in parentheses, calculated as $(k_{E_p^0}^{AOP} - k_{E_p^0}^{UV}) / k_{E_p^0}^{AOP}$.

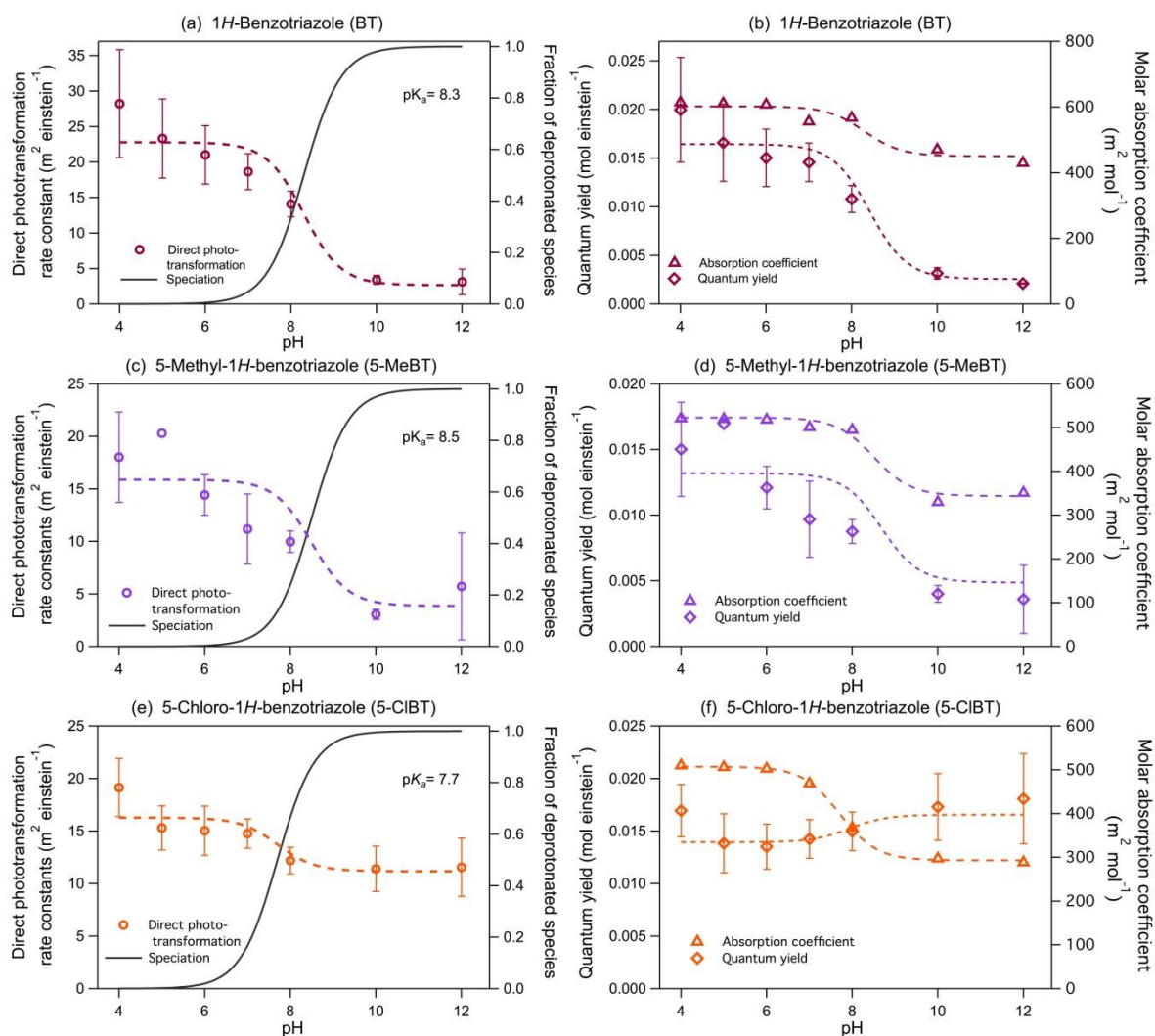
Figure 1

Figure 1. Direct phototransformation of benzotriazoles: Apparent photon fluence-based rate constants ($k_{E_p^0}^{dp,app}$, left panels: a, c, e), molar absorption coefficients (ϵ_{254nm}^{app} , right panels: b, d, f) and quantum yields ($\Phi_{254nm}^{dp,app}$, right panels: b, d, f) as a function of pH. The continuous lines (left panels: a, c, e) represent the fractions of deprotonated species, the dotted lines are best fit functions determined as described in the text.

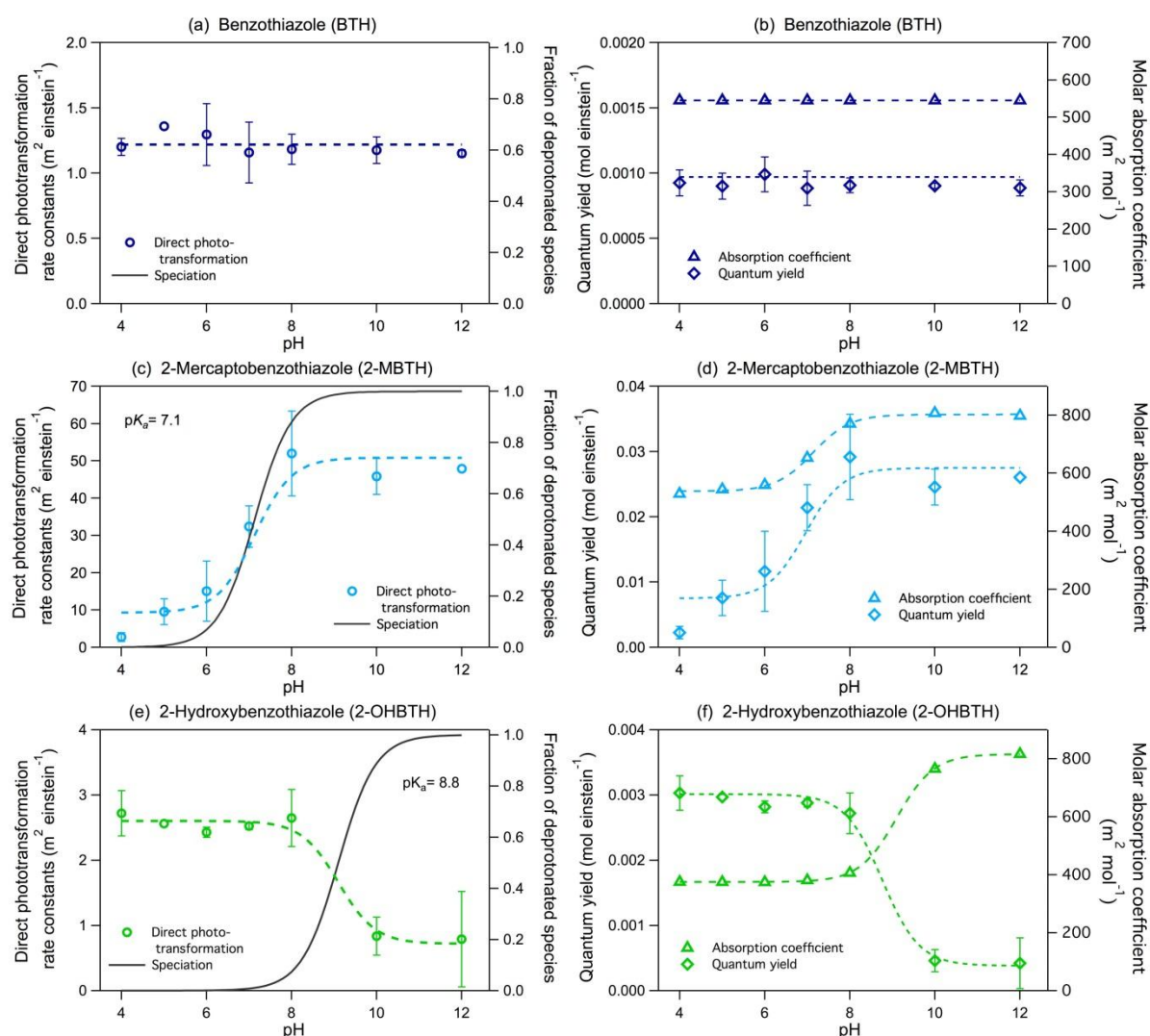
Figure 2

Figure 2. Direct phototransformation of benzothiazoles: Apparent photon fluence-based rate constants ($k_{E_p}^{dp,app}$, left panels: a, c, e), molar absorption coefficients (ϵ_{254nm}^{app} , right panels: b, d, f) and quantum yields ($\Phi_{254nm}^{dp,app}$, right panels: b, d, f) as a function of pH. The continuous lines (left panels: a, c, e) represent the fractions of deprotonated species, the dotted lines are best fit functions determined as described in the text.

Figure 3

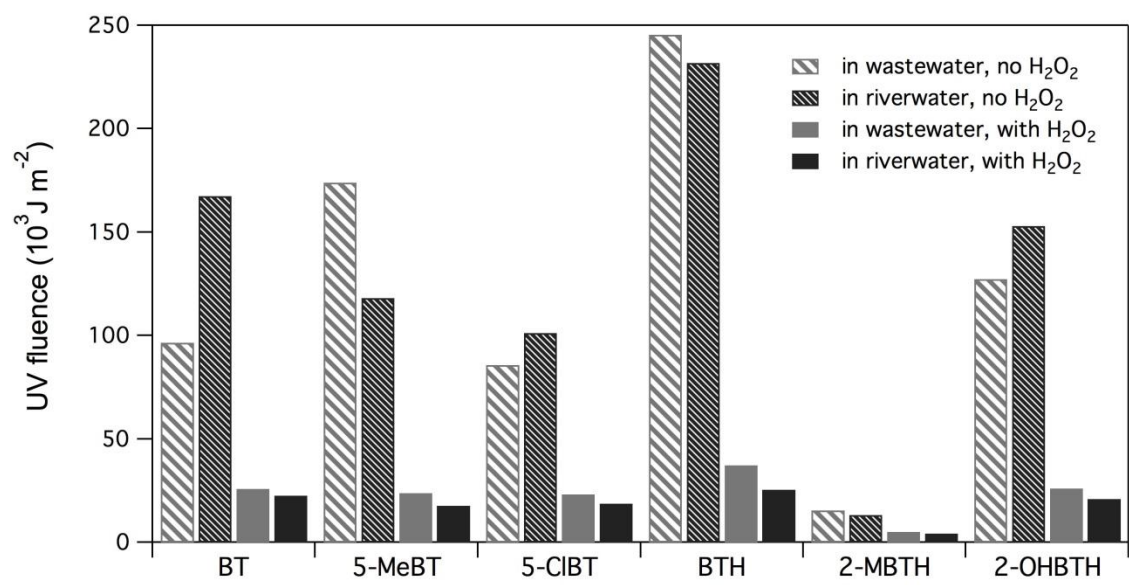


Figure 3. Required UV fluence to achieve a 90% removal ($H_{r,90\%}$) of selected benzotriazoles and benzothiazoles for treatment with UV and UV/ H_2O_2 ($[\text{H}_2\text{O}_2] = 5 \text{ mg L}^{-1}$) of the studied wastewater and river water.

Electronic Supplementary Material (for online publication only)

[Click here to download Electronic Supplementary Material \(for online publication only\): Bahnmler_BTs&BTHs-SI_SC03Oct2014.](#)